J Mol Model (2013) 19:1251–1258
DOI 10.1007/s00894-012-1651-5

ORIGINAL PAPER

Effect of varying the 1–4 intramolecular scaling factor in atomistic simulations of long-chain N-alkanes with the OPLS-AA model

Xianggui Ye · Shengting Cui · Valmor F. de Almeida · Bamin Khomami

Received: 5 September 2012 / Accepted: 14 October 2012 / Published online: 20 November 2012

Abstract A comprehensive molecular dynamics simulation study of n-alkanes using the optimized potential for liquid simulation with all-atoms (OPLS-AA) force field at ambient condition has been performed. Our results indicate that while simulations with the OPLS-AA force field accurately predict the liquid state mass density for n-alkanes with carbon number equal or less than 10, for n-alkanes with carbon number equal or exceeding 12, the OPLS-AA force field with the standard scaling factor for the 1–4 intramolecular Van der Waals and electrostatic interaction gives rise to a quasi-crystalline structure. We found that accurate predictions of the liquid state properties are obtained by successively reducing the aforementioned scaling factor for each increase of the carbon number beyond n-dodecane. To better understand the effects of reducing the scaling factor, its influence on the torsion potential profile, and the corresponding gauche-trans conformer distribution, heat of vaporization, melting point, and self-diffusion coefficient for n-dodecane were investigated. This relatively simple procedure enables more accurate predictions of the thermo-physical properties of longer n-alkanes.

Keywords Alkanes · Chain stiffness · Intramolecular interaction · Molecular dynamics · OPLS · Scaling factor

Electronic supplementary material The online version of this article (doi:10.1007/s00894-012-1651-5) contains supplementary material, which is available to authorized users.

X. Ye · S. Cui (✉) · B. Khomami
Materials Research and Innovative Laboratory (MRAIL),
Department of Chemical and Biomolecular Engineering,
University of Tennessee,
Knoxville, TN 37996, USA
e-mail: scui@utk.edu

B. Khomami (✉)
Sustainable Energy and Research Center, University of Tennessee,
Knoxville, TN 37996, USA
e-mail: bkhomami@utk.edu

V. F. de Almeida
Oak Ridge National Laboratory,
Oak Ridge, TN 37831-6181, USA

Introduction

Force field development is a vital part of molecular modeling for the study of liquid systems. The most widely used force field models include CHARMM [1], AMBER [2], and OPLS [3, 4], among which the OPLS model, in particular, was optimized to predict properties of liquids. Although the force field parameters were developed through ab initio electronic structure calculations and carefully calibrated with experimental data for prototypical molecular fragments, less rigorous choices have been made for some of the non-bonded intramolecular interactions, such as the 1–4 intramolecular van der Waals and Coulombic interactions. Often, an *ad hoc* approach has been used to reduce the interaction between the 1–4 intramolecular atom pairs [1–4]. In an early version, for example, AMBER used scaling factors (SF) 1/2 for both the van der Waals and Coulombic interactions [5]. With refined partial atomic charges determined through fitting to the electrostatic potential, AMBER currently uses scaling factors (SF) 1/2 and 1/1.2 for the van der Waals and Coulombic interactions, respectively [2]. In the OPLS-AA force field model, a scaling factor of 1/2 is commonly used for both types of interaction, although scaling factors as low as 1/8 has been used in the past [6]. The physical bases for such scaling are to account for the reduced short-range interaction which has been partially included in the torsion potential, as well as the lack of polarizability in the classical potential models [2, 5].

Alkanes are important in many industrial processes, e.g., polyethylene, is the most widely used plastic [7]. Hence, alkanes are one of the most widely studied organic liquids via atomistic simulations both for their practical importance

as well as serving as a prototype for exploring the influence of chain-length on the thermodynamic and transport properties of macromolecules [8]. Recent work on atomistic modeling of surface adsorption of monolayer alkanes on a graphite surface utilizing the CHARMM force field has demonstrated that the surface freezing temperature of alkanes is dependent on the SF [9]. Freezing of alkanes near a water-alkane interface has also been observed [10]. These studies clearly raise the question of whether such a tendency for ordering in alkanes is a result of surface or interfacial effects, or excessive chain stiffness inherent in the force field model. A definitive clarification of such effect is especially important for longer chains as this effect is cumulatively enhanced. More recently, Siu et al. [11] motivated by their observation that the OPLS-AA force field results in a liquid-to-gel-phase transition for pentadecane well above 300 K, have reparameterized the torsion potential and adjusted Lennard-Jones (LJ) energy parameter for methylene hydrogen and all partial atomic charges. Since the torsional potentials consist of a cosine series plus the 1,4-nonbonded interaction (Coulombic and Lennard-Jones), it is reasonable to assume that tuning the 1,4 intramolecular interaction should allow for more realistic predictions of the thermo-physical properties of long-chain alknaes. To this end, in this paper we elucidate the effect of the SF on the variation of the torsion potential profile, and its corresponding impact on the gauche-trans conformation distribution, heat of vaporization, melting point, and self-diffusion coefficient for n-dodecane, to unambiguously delimit the applicable parameter space for the SF in the molecular simulation study of liquid alkanes.

Methods

We have thus carried out extensive molecular dynamic simulations of pure n-alkane liquids in the NPT ensemble at 25 °C and 1 bar running LAMMPS [12] with the Verlet integrator and a Nosé-Hoover thermostat and barostat (with a temperature damping parameter 0.1 ps, and a pressure damping parameter 1 ps) using a time step of 1 fs. The systems studied consisted of 500 alkane molecules in a cubic simulation box unless otherwise noted. The OPLS-AA force field [4] with an updated torsion potential [5, 13] was used. A cutoff distance 12 Å was used for the Lennard-Jones interaction and standard long-range correction was applied. The particle − particle particle − mesh method [14] with a real space truncation distance 12 Å and an accuracy of 10^{-6} was used to treat the electrostatic interactions.

To eliminate the possibility of any artifact due to initial configuration and simulation method, two different methods have been used to generate the initial configuration. Specifically, in one case, the system was equilibrated using an NVT ensemble at liquid density and temperature of 1000 °C, followed by re-equilibration in an NPT ensemble under ambient conditions. It is noted that the approach is very similar to the procedure used in prior MC simulations [5]. In the second approach, the equilibrated configuration from a calculation with lower SF where the system is in a liquid state under ambient conditions was used as the initial configuration for a calculation with a higher SF. Both methods lead to the same final state condition, hence, excluding the possibility of kinetically trapped states. In addition, although the reported simulations results in this paper are based on NPT ensembles, test simulations in an NVT ensemble for n-dodecane with SF=0.5 were also performed with varying thermostat time constant for which the formation of quasi-crystalline structures were also observed. This further supports the fact that the observation of quasi-crystalline structures with standard SF is not an artifact of initial configuration or simulation method used.

Results and discussion

Quasi-crystalline structure for N-dodecane at ambient condition

The time evolution of the computed mass density and end-to-end distance, R_{ee}, of n-dodecane from an initial disordered liquid state utilizing the OPLS-AA force field with the standard SF=0.5 are shown in Fig. 1a. The inset in this figure clearly demonstrates that below 1 ns, which is roughly equivalent to the Monte Carlo simulation duration in ref. 5 (this assertion is based on the roughly estimated equivalence of n MC moves to a one MD time step, where n is the number of molecules), the computed mass density appears to have reached equilibrium, while the R_{ee} exhibits a slight increase. Thus, if an insufficiently long simulation is performed, an apparent liquid state mass density and end-to-end distance is obtained. However, at longer times, the mass density and the R_{ee} continue to rise until reaching a new plateau at about 10 ns. The R_{ee} for the new plateau is about 13.83 Å, nearly equal to the length of the fully extended n-dodecane, 14.07 Å [5]. A snapshot of the corresponding microscopic structure at the end of the simulation (Fig. 1b) clearly shows the system has transitioned into a quasi-crystalline state. To ensure that this unrealistic transition is not caused by the relatively small size of the system, computation with 4000 n-dodecane molecules using SF equal to 0.5 were also performed. A similar transition was also observed in the larger system (Fig. 1c).

Effect of varying the scaling factor

To understand the cause for appearance of the quasi-crystalline phase in n-dodecane at ambient condition, we

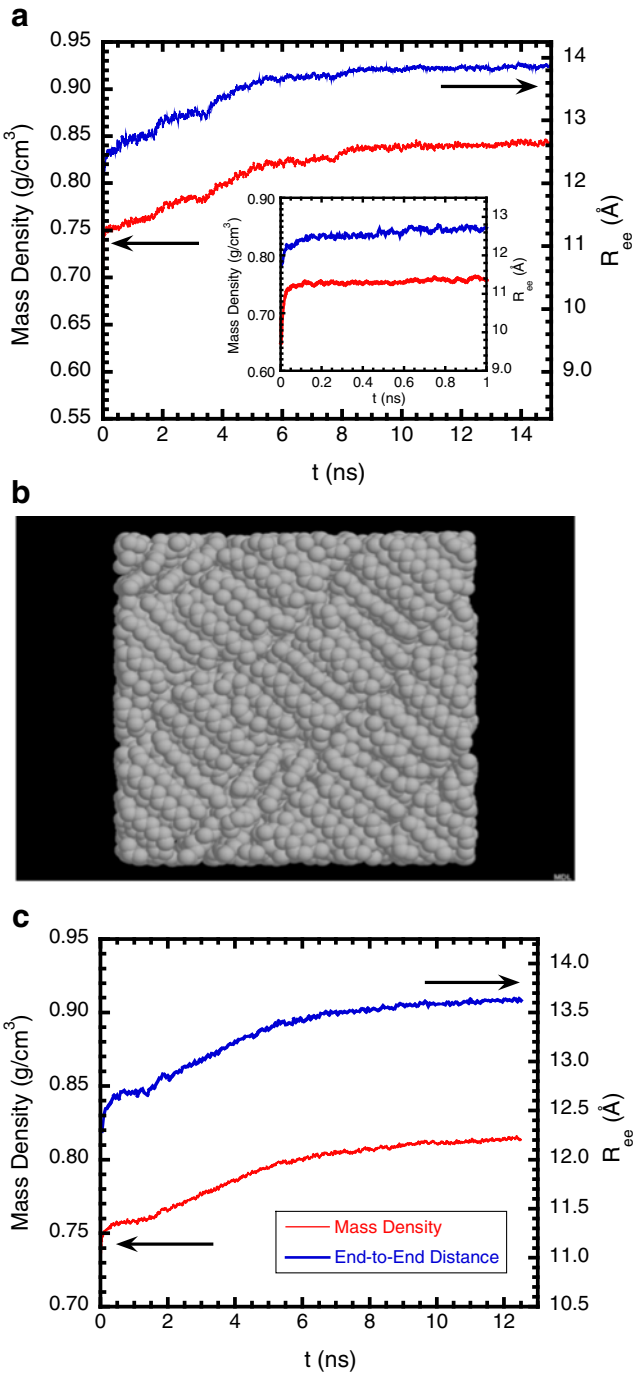

Fig. 1 **a** Mass density (red) and end-to-end distance (blue) as a function of time for n-dodecane with SF=0.5. The inset is a closer view for the initial 1 ns. **b** Snapshot of the configuration at 15 ns. Only carbon backbones are shown. **c** Mass density (red) and end-to-end distance (blue) as a function of time for n-dodecane with SF=0.5 for 4000 molecules in the system (T=25 °C, P=1 bar)

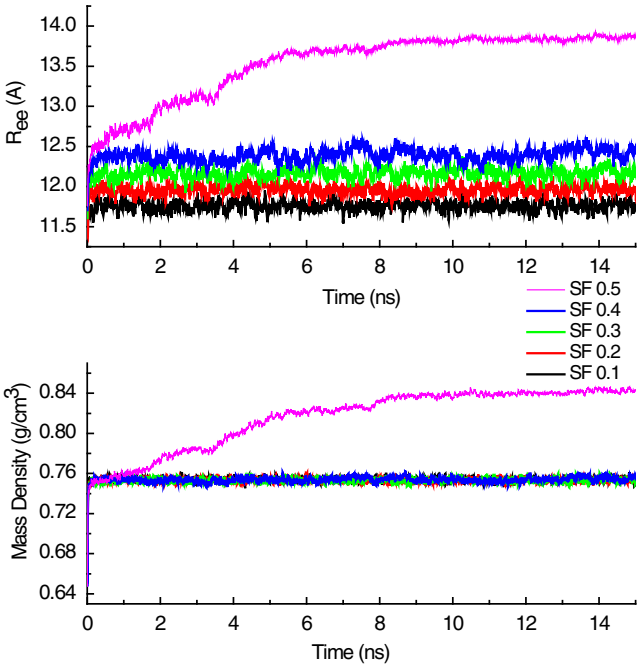

Fig. 2 Mass density and end-to-end distance for n-dodecane as a function of time (T=25 °C, P=1 bar). The mass density for SF=0.1 to 0.4 overlaps each other

have examined the effect of varying the scaling factor for the intramolecular 1–4 interaction used in the OPLS-AA force field. Figure 2 shows the mass density and chain end-to-end distance, R_{ee}, for n-dodecane as a function of time for varying SF from 0.1 to 0.5. When a scaling factor between 0.1 and 0.4 is used, the mass density and R_{ee} rapidly (less than 0.2 ns) reach their equilibrium values and maintain their respective values for the reminder of the 15 ns simulation time. For SF=0.5, in comparison, both the mass density and the R_{ee} continuously increase over a time duration about 10 ns.

The average mass density and R_{ee} calculated as a function of SF are presented in Fig. 3. It is seen that for SF equal and less than 0.4, the mass density variations are insignificant while R_{ee} shows a gradual increase with SF. However, from SF=0.4 to 0.5, a large jump occurs for both the R_{ee} and the mass density. Specifically, as SF is increased from 0.1 to 0.4, R_{ee} gradually increases with a total change of ~6 %, however, a drastic increase is observed in R_{ee} (>10 %) between SF of 0.4 and 0.5. The corresponding mass density shows a similar large increase from 0.753 to 0.824 g/cm^3, a 9.4 % increase, as a result of ordered packing of the chains. The commensurate increase in the mass density and R_{ee} (see also Fig. 2) suggests a close correlation between the two quantities, where the latter is intimately related to the chain stiffness and thus to the 1–4 intramolecular interaction through the scaling factor (see more detailed discussion in section Chain length dependence).

To precisely quantify the molecular order in the system, the time evolutions of the orientation order parameters are

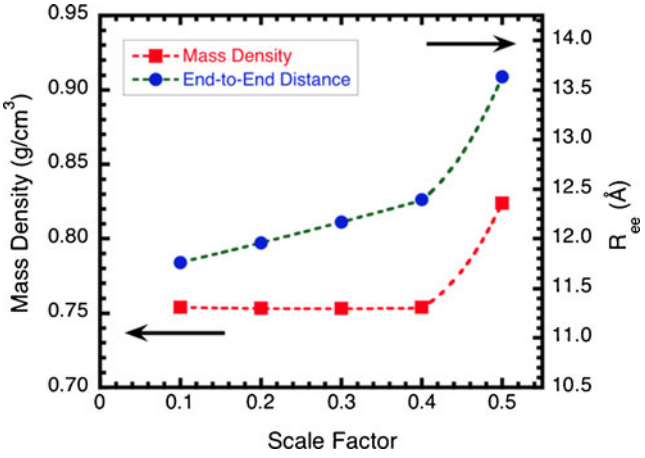

Fig. 3 Mass density and end-to-end distance of n-dodecane as a function of the SF: the red squares represent the mass density, and the blue circles correspond to the chain end-to-end distance. Arrows indicate the respective axis for the two quantities

computed (see Fig. 4) from the second rank order tensor, defined as [15–17]:

$$S = \frac{3}{2}\left\langle \frac{1}{N}\sum_{i=1}^{N}\left(\hat{\boldsymbol{r}}\,\hat{\boldsymbol{r}} - \frac{1}{3}\boldsymbol{I}\right)\right\rangle \quad (1)$$

where S is a second rank tensor, $\hat{\mathbf{r}}$ is a unit vector along the end-to-end vector, $\boldsymbol{I}$ is a second rank unit tensor, N is the number of molecules, and the summation runs through all the molecules in the system. Three order parameters which quantitatively characterize the extent of the orientation order in the system can be extracted from S. Figure 4 shows these orientation order parameters as a function of time for n-dodecane with SF=0.1 to 0.5. Specifically, the three orientation order parameters for systems with SF from 0.1 to 0.4 during the 15 ns simulation are very close to zero, which is in accord with a disordered isotropic liquid. At SF 0.5 the order parameters are initially very close to zero, suggesting the initial configuration is a disordered isotropic liquid, however, at intermediate times, the largest orientation parameter, χ_1, increases (accompanied by the corresponding decrease of χ_2 and χ_3) until about 5 ns, and then slowly reaches a plateau in a very similar fashion as the computed mass density and R_{ee} (shown in Fig. 1a), indicating the presence of preferred chain orientation. Together, the results shown in Figs. 1 and 4 demonstrate that when using a SF=0.5, the OPLS-AA force field overestimates the chain stiffness for n-dodecane and produces an unrealistic quasi-crystalline structure where a liquid is expected.

Chain length dependence

The foregoing prompted us to carry out a systematic study of the effect of SF on the structural order of n-alkanes of various chain lengths. Specifically, three additional n-alkanes, namely, n-decane, n-tetradecane, and n-hexadecane were investigated. Varying the SF in atomistic simulations of each n-alkane has enabled us to probe the boundary between the predicted quasi-crystalline and disordered liquid regions for n-decane to n-hexadecane which is depicted in Fig. 5. It is

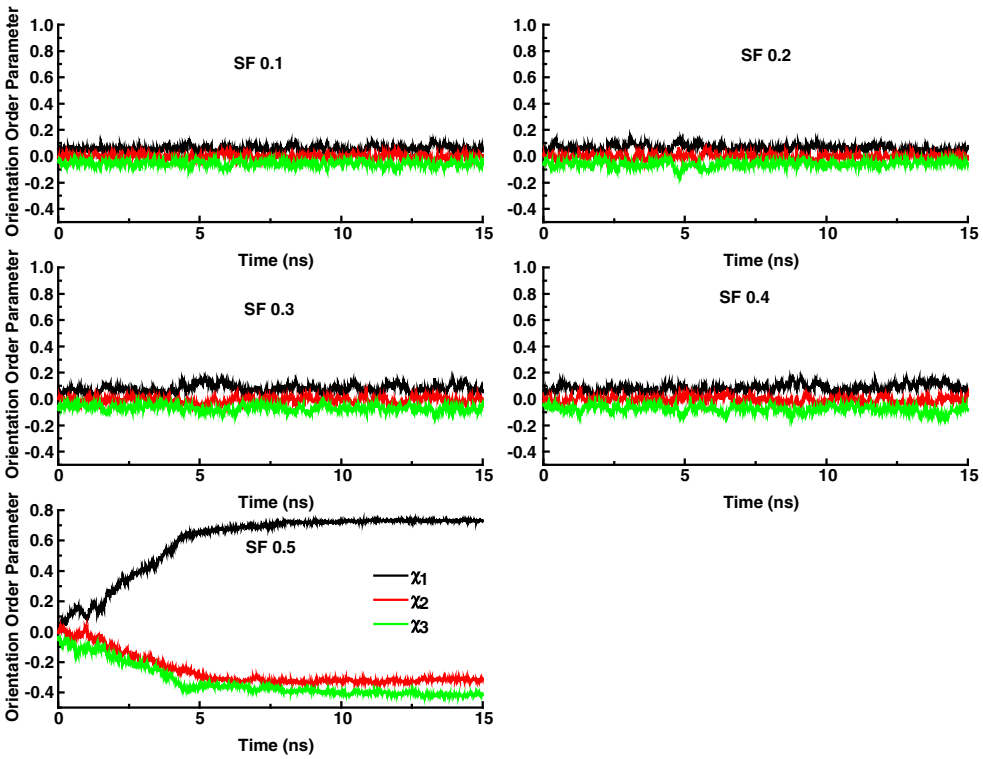

Fig. 4 Orientation order parameters for n-dodecane for SF=0.1, 0.2, 0.3, 0.4, and 0.5. They clearly show the formation of an ordered crystalline state for SF=0.5

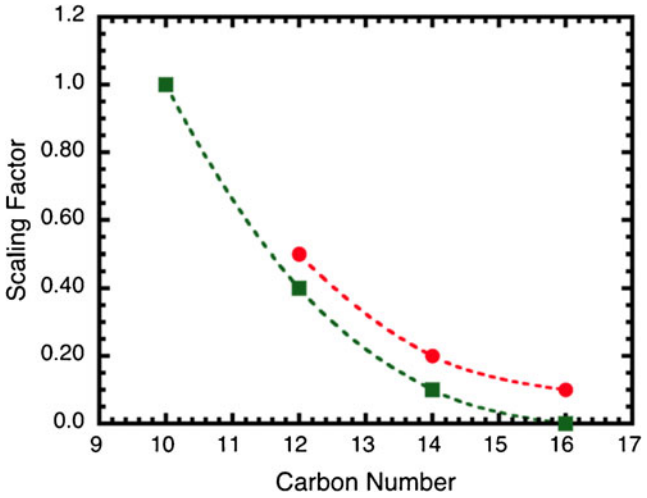

Fig. 5 The computed boundary between the quasicrystalline and the liquid state for n-alkanes containing 10 to 16 carbons. The lines are a guide to the eyes. When the SF is above the red symbols, the n-alkanes are in a quasicrystalline phase. When the SF is below the green symbols, the n-alkanes are in a disordered phase

experimentally known that under ambient conditions (25 °C, 1 bar), n-decane, n-dodecane, n-tetradecane, and n-hexadecane are disordered liquids, with melting temperature of −30, −9.6, 5.5, 18 °C, respectively (http://webbook.nist.gov/chemistry/). Using the standard SF=0.5, however, the simulation give rise to a quasi-crysralline structure in all cases with the exception of n-decane. The n-decane was found to remain in the liquid state even for SF as high as 1.0.

We found that as the number of carbons in the chain increases, reduced SF values had to be used to correctly model the phase state of the longer alkanes. Specifically, for n-dodecane, n-tetradecane, and n-hexadecane, a quasi-crystalline state is observed for SF=0.5, 0.2, and 0.1, respectively; whereas the system remains in liquid state for SF=0.4, 0.1, and 0, respectively (see Fig. 2, and Supplemental materials Figs. 9–11). Therefore, the boundary for crossing over from one state to the other should fall between the two aforementioned SF values for each n-alkane. In addition, similar to n-dodecane the computed mass density of longer chain n-alkanes in the liquid phase is insensitive to variation of the SF.

Dependence of torsion potential profiles, thermodynamic and transport properties on SF

Torsion potential profile

In this section, we discuss in detail the consequences of adjusting the 1–4 intramolecular scaling factor within the OPLS-AA framework and analyze how the various interactions affect the flexibility of n-alkanes. In Fig. 6, we show the torsion potential profile of n-dodecane with varying SF from 0.5 to 0, calculated at temperature 25 °C at very low

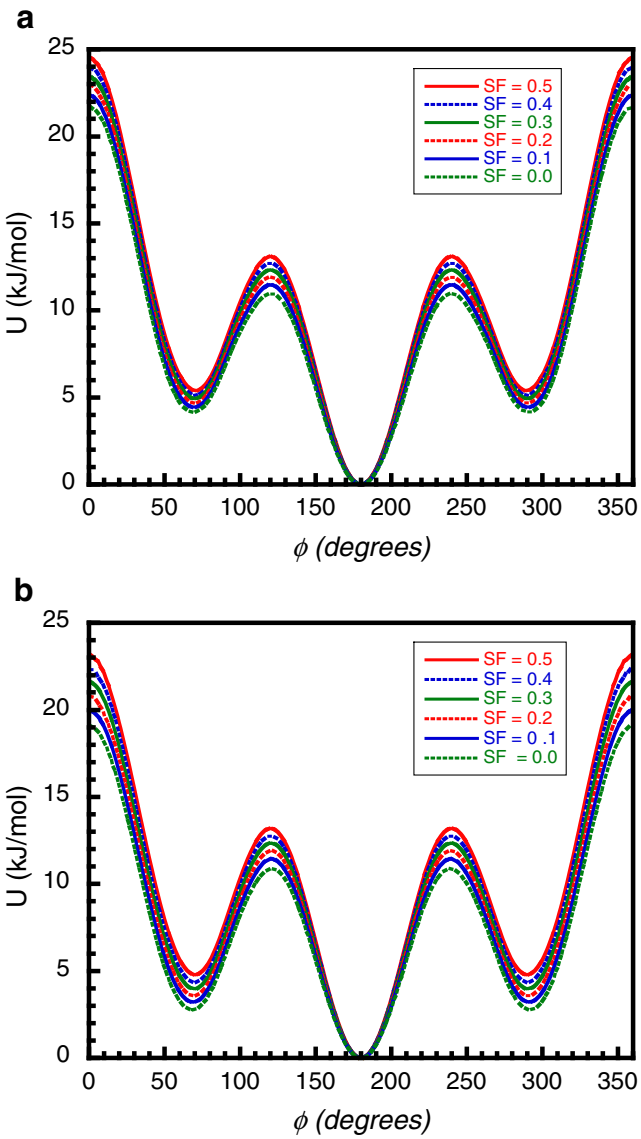

Fig. 6 Comparison of torsion potential profiles for n-dodecane in gas phase as a function of the 1–4 intramolecular scaling factor. **a** Torsion profile for the interior dihedral: CH_2-CH_2-CH_2-CH_2. **b** Torsion potential profile for the terminal dihedral: CH_3-CH_2-CH_2-CH_2

gas density of 1000th of its liquid density. The potential profiles were produced by calculating the Boltzmann population probability distribution for the dihedral angles. To simulate dilute gas in the torsion profile calculations, we have retained only the short-range repulsive interaction for the intermolecular interaction (the repulsive term of the Lennard-Jones potential). Thus, the intermolecular interaction energy is negligible compared to the intramolecular interaction energy. This models the ideal gas case where intermolecular interaction is negligible and gives the same results as single molecule simulation but with better statistics.

In the figure, we show the torsion profiles corresponding to the two types of backbone torsions: CH_2-CH_2-CH_2-CH_2 and CH_3-CH_2-CH_2-CH_2. It is noted that for both types of

dihedral angle, the minimum of the potential well for gauche conformation systematically decreases with the SF (by 1.2 kJmol^{-1} for the former and 2.0 kJmol^{-1} for the latter) and so does the gauche-trans transition barrier (by 2.1 kJ mol^{-1} for the former and 2.3 kJmol^{-1} for the latter), suggesting that the molecule becomes more flexible with each successive reduction of the scaling factor. It is also noted that the gauche well depth for the CH_3-CH_2-CH_2-CH_2 is lower by about 0.6–1.4 kJmol^{-1} than that of the CH_2-CH_2-CH_2-CH_2 (with the larger value corresponding to the smallest SF), which explains why the calculated fraction of gauche conformers for n-dodecane is higher for the terminal dihedrals than for the interior (see Fig. 8 below).

We also examined the effect of separately reducing the SF for the LJ interaction and the electrostatic interaction. This is shown in Fig. 7 for the interior dihedral: CH_2-CH_2-CH_2-CH_2. In Fig. 7a we compare the cases of the 1–4 LJ interaction SF=0.5, 0.2, and 0.0 while keeping the electrostatic interaction scaling factor at 0.5. It is seen that the reduction of the LJ scaling factor has little effect on the well depth but reduces the gauche-trans transition barrier. Figure 7b compares the effect of reducing the electrostatic scaling factor but keeping the LJ SF=0.5. It shows that the main effect of the electrostatic interaction is to lower the well depth for the gauche conformation, while at the same time slightly lowering the gauche-trans transition barrier. The torsion potential profile for the terminal dihedral: CH_3-CH_2-CH_2-CH_2 show similar behavior (see Supplemental materials, Figs. 12 and 13).

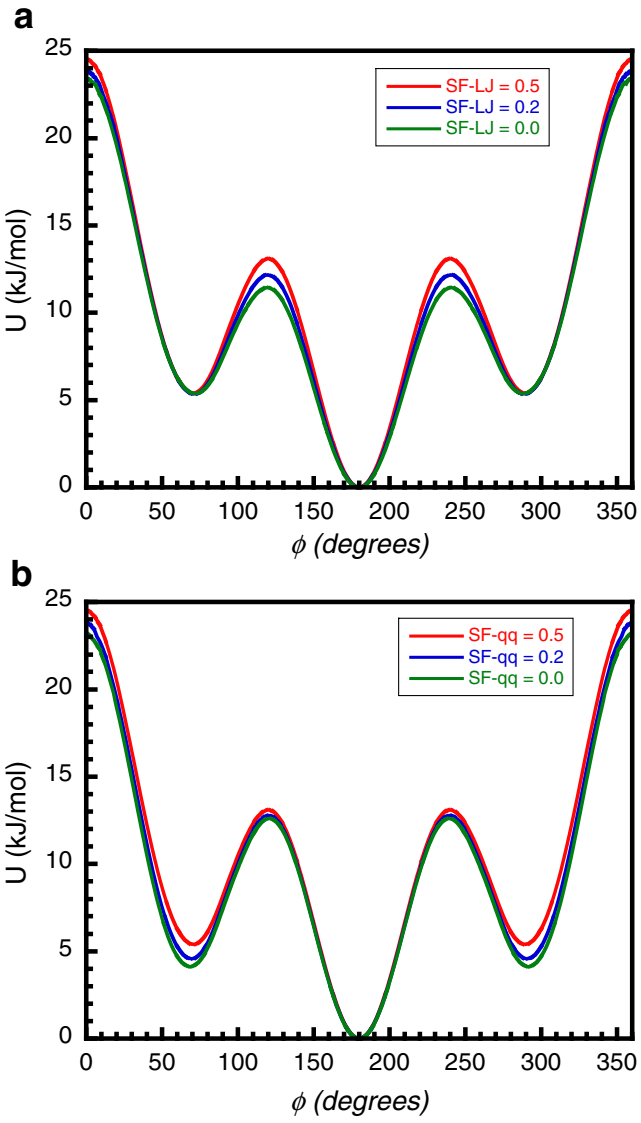

Fig. 7 Comparison of torsion potential profile for n-dodecane for the interior dihedral: CH_2-CH_2-CH_2-CH_2 in gas phase for varying 1–4 intramolecular scaling factor: **a** for either only the Lennard-Jones; or (**b**) the electrostatic interaction is varied while keeping the other part of SF 0.5 unchanged

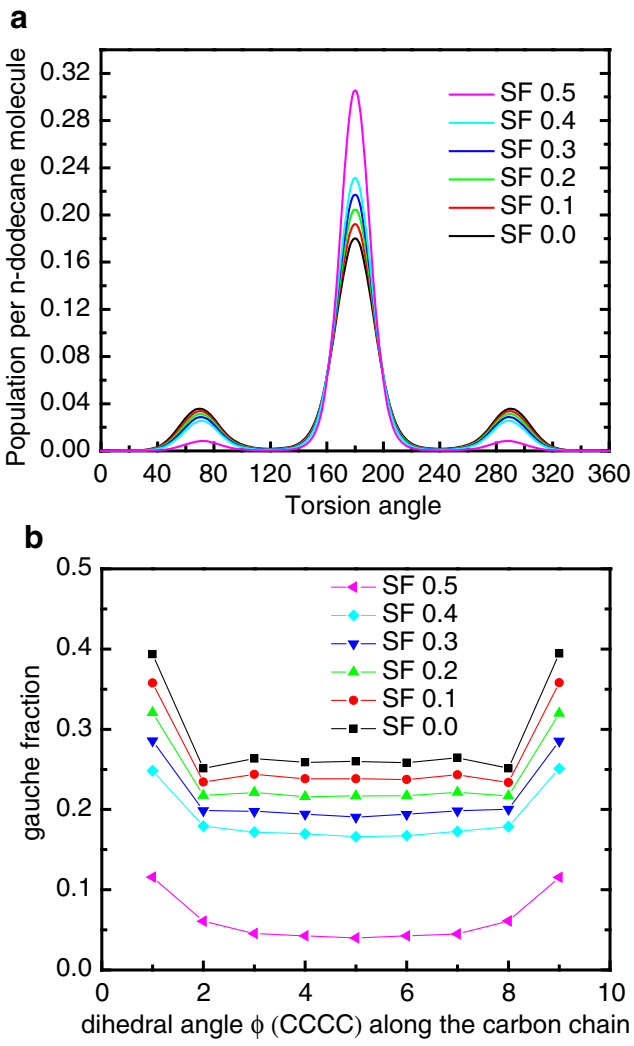

Fig. 8 **a** Dihedral angle distributions per n-dodecane in condense phase with different 1–4 interaction scaling factor. **b** Gauche-trans fractions of dodecane in condense phase as a function of dihedral angle along the carbon chain with different 1–4 interaction scaling factor

To investigate the SF effect on dihedral angle in condensed phase (liquid or quasicrystalline phase when it occurs) at ambient condition, we calculated the population distribution in condensed phase as a function of dihedral angle averaged over all dihedral angles for n-dodecane (shown in Fig. 8a), and the fraction of the gauche conformers for each dihedral angle along the backbone of the n-dodecane (shown in Fig. 8b). Clearly, there are significant changes in dihedral angle distributions per n-dodecane and gauche-trans fractions of dodecane in condense phase when SF decreases from 0.5 to 0.4 due to quasi-crystallization at SF 0.5. Consistent with the torsion profile analysis in gas phase, the gauche population increases with each consecutive decrease of the SF, and correspondingly, the fraction of dihedrals with gauche conformation increase. Therefore, the n-dodecane molecule becomes increasingly more flexible. For the lowest SF used here, the fraction of the gauche conformation is close to but slightly below those predicted by other force field models [11]. There are limited experimental data available on the fraction of gauche-trans distribution for n-alkanes in liquid which diverges considerably, ranging from 0.24 to 0.43 [18–24]. It has been noted that because of experimental difficulty, the ratio of *trans*/*gauche* conformers concentration at room temperature can be predicted only with an error of approximately 40 % [25]. In comparison, the predicted fraction gauche conformation here is close to the lower range of the experimental values. With a clear understanding of the effect of reducing the SF, the simplicity of the flexibility of the approach here make it useful to adjust the existing models to accurately predict thermophysical properties of systems for longer n-alkanes where deviation from experiment, such as melting temperature, becomes more pronounced.

Thermodynamic and transport properties

In Table 1, we present other properties, including: heat of vaporization, and the self-diffusion coefficient, as well as the mass density, and end-to-end distance of n-dodecane. The Heat of vaporization is calculated using the standard formula:

$$\Delta H_{vap} = E(g) - E(l) + RT \quad (2)$$

where $E(g)$ and $E(l)$ are the potential energy of the molecules in the gas and liquid phase, respectively. The liquid phase potential energy is calculated from our standard MD simulation above. The gas phase intramolecular potential energy is calculated from simulations of a gas obtained by diluting the liquid phase 5095 times. We have checked that the density was sufficiently low by further diluting the gas to 15,868 times and that there is no density dependence. In addition, we performed MD calculations for a gas phase of 1000 times dilution where only short-range repulsive intermolecular interaction (in the form of the repulsive term of the Lennard-Jones potential) is allowed between different molecules, similar to non-interacting gas phase, all calculations give the same results within statistical uncertainty.

As can be seen in Table 1, reducing the SF has the effect of lowering the heat of vaporization and bringing the quantity closer to the experimental value. As shown in Fig. 8a, the gauche conformer fraction increases with reducing the SF. Physically the gauche conformers in the liquid phase reduce the strength of cohesion of molecules in the liquid phase and thus make it easier to evaporate.

The self-diffusion coefficient was calculated from the ensemble average of the mean square displacement of the center of mass motion of the n-dodecane molecules. It is seen in Table 1 that with each successive reduction of the SF, the diffusion coefficient increases. This is expected as the n-dodecane molecules become more flexible with the reduction of the SF, hence it is easier for the molecules to migrate through between the other molecules. From SF=0.5 to SF=0.0, the diffusion coefficient increases from $(4.644\pm 0.234)\times 10^{-10}$ to $(5.747\pm 0.156)\times 10^{-10}$ m^2/s, compared to the experimental value of 8.71×10^{-10} m^2/s [27]. The best value obtained here for SF=0.0 gives a comparable and slightly better agreement than that of Siu et al. [11]. Note that the self-diffusion coefficient may increase with the system size by 10–24 % as reported [11, 28, 29]. Therefore,

Table 1 Heats of vaporization (ΔH_{vap}), self-diffusion coefficient (D_s), melting point, mass density, and end-to-end distance of n-dodecane using the OPLS-AA parameters as a function of 1,4 interaction scaling factors

Scaling factor	ΔH_{vap} (kJ/mol)	D_s (10^{-10} m^2/s)	Melting point (K)	Mass density (g/cm^3)	End-to-end distance (Å)
0.5	> 85.60	~0	306±1	0.8240±0.0272	13.63±0.37
0.4	65.73±0.67	4.644±0.234	ND[c]	0.7540±0.0034	12.39±0.07
0.3	64.94±0.75	4.883 ±0.208	ND[c]	0.7531±0.0033	12.17±0.07
0.2	64.14±0.67	5.351 ±0.256	285±1	0.7533±0.0031	11.96±0.06
0.1	63.68±0.63	5.540 ±0.186	ND[c]	0.7541±0.0030	11.76±0.06
0.0	63.47±0.59	5.747 ±0.156	261±1	0.7555±0.0019	11.57±0.06
expt.	61.287[a]	8.71[b]	263.356[a]	0.74518[a]	

[a]data from ref. [26]

[b]data from ref. [27]

[c]not determined

considering the finite size effect, our self-diffusion coefficient will be more comparable with the experimental data.

The melting points of n-dodecane with different SFs are also shown in Table 1. To obtain the melting points, we performed a series of simulations for a range of temperatures, monitoring the density and structure development of the system with non-quasi-crystalline initial configuration. Clearly, with the gradual decrease of the SF, the melting point decreases accordingly. At SF 0.0, the simulated melting point agrees well with the experimental one (263.356 K) [26]. With smaller SF, the n-dodecane molecule is more flexible. Therefore, the flexible molecule requires less heat to melt, and the melting point is lowered.

Conclusions

Extensive molecular dynamics simulations of n-alkanes with carbon numbers ranging from 10 to 16 at ambient condition using the OPLS-AA have been performed. For n-alkanes with carbon number equal or less than 10, simulations accurately predict the phase and the mass density of the system. For n-alkanes with carbon number equal or greater than 12, however, we found that the standard scaling factor for the 1–4 intramolecular van der Waals and electrostatic interactions used in the model causes the n-alkanes to transition into a quasi-crystalline state where a liquid state is expected. By reducing the scaling factor, the expected liquid state is restored and the predicted mass density agrees well with experiment. Moreover, the predicted mass density is relatively insensitive to the value of the scaling factor as long as the SF is below the transition point. However, as the n-alkane chain length increases beyond 12 carbon atoms, a smaller SF as low as SF =0.0 is recommended to maintain the liquid state for longer alkanes at the ambient condition.

We have analyzed the effect of reducing the scaling factor based on the original OPLS-AA force field. We show that reducing the scaling factor improves all the commonly encountered thermophysical properties of liquid n-dodecane. It is reasonable to expect this is the case for other long n-alkanes. With this clear understanding of the effect of the scaling factor, this simple approach here can be used to further improve other all-atom models for n-alkanes, and to fine-tune the models to correct the deviation of the predictions from experimental data for longer n-alkanes on properties such as melting temperature and self-diffusion coefficient on which the chain flexibility has an important effect.

Acknowledgments This work was supported by the US Department of Energy, Office of Nuclear Energy under the Nuclear Energy University Program (DOE-NEUP), contract number: DE-AC07-051D14517. Computing resources used at the Center for Advanced Modeling and Simulation at the Idaho National Laboratory through a collaboration with the Nuclear Energy Advanced Modeling and Simulation program of the Nuclear Energy Office of DOE are greatly appreciated. The Oak Ridge National Laboratory is managed by UT-Battelle, LLC for the DOE under contract No. DE-AC05-00OR22725.

References

1. MacKerell AD, Bashford D, Bellott M et al. (1998) J Phys Chem B 102:3586–3616
2. Cornell WD, Cieplak P, Bayly CI, Gould IR, Merz KM, Ferguson DM, Spellmeyer DC, Fox T, Caldwell JW, Kollman PA (1995) J Am Chem Soc 117:5179–5197
3. Jorgensen WL, TiradoRives J (1988) J Am Chem Soc 110:1657–1666
4. Jorgensen WL, Maxwell DS, TiradoRives J (1996) J Am Chem Soc 118:11225–11236
5. Weiner SJ, Kollman PA, Case DA, Singh UC, Ghio C, Alagona G, Profeta S, Weiner P (1984) J Am Chem Soc 106:765–784
6. Thomas LL, Christakis TJ, Jorgensen WL (2006) J Phys Chem B 110:21198–21204
7. Piringer OG, Baner AL (2008) Plastic packaging: interactions with food and pharmaceuticals, 2nd edn. Wiley-VCH, Weinheim
8. Ungerer P, Nieto-Draghi C, Rousseau B, Ahunbay G, Lachet V (2007) J Mol Liq 134:71–89
9. Firlej L, Kuchta B, Roth MW, Wexler C (2011) J Mol Model 17:811–816
10. Bresme F, Chacon E, Tarazona P (2010) Mol Phys 108:1887–1898
11. Siu SWI, Pluhackova K, Boeckmann RA (2012) J Chem Theor Comp 8:1459–1470. During the preparation of this manuscript, the paper by Siu et al. appeared that used a different approach to improve the performance of the OPLS-AA potential
12. Plimpton S (1995) J Comp Phys 117:1–19. URL:http://lammps.sandia.gov/
13. Price ML, Ostrovsky D, Jorgensen WL (2001) J Comp Chem 22:1340–1352
14. Darden T, York D, Pedersen D (1993) J Chem Phys 98:10089–10092
15. Chandrasekhar S (1992) Liquid Crystals, 2nd edn. Cambridge University Press, Cambridge
16. de Gennes PG, Prost J (1993) The Physics of Liquid Cyrstal, 2nd edn. Clarendon, Oxford
17. Cui ST, Gupta SA, Cummings PT, Cochran HD (1996) J Chem Phys 105:1214–1220
18. Menger FM, D'Angelo LL (1988) J Am Chem Soc 110:8241–8244
19. Casal HL, Yang PW, Mantsch HH (1986) Can J Chem 64:1544–1547
20. Casal HL, Mantsch HH (1989) J Mol Struct 192:41–45
21. Casal HL, Mantsch HH (1989) J Mol Struct 213:328–328
22. Holler F, Callis JB (1989) J Phys Chem 93:2053–2058
23. Deleuze MS, Pang WN, Salam A, Shang RC (2001) J Am Chem Soc 123:4049–4061
24. Compton DAC, Montero S, Murphy WF (1980) J Phys Chem 84:3587–3591
25. Balabin RM (2009) J Phys Chem A 113:1012–1019
26. Riddick JA, Bunger WB, Sakano TK (1986) Techniques of Chemistry, Vol. II, 4th edn, Organic Solvents, Physical Properties and Methods of Purification. Wiley, New York
27. Tofts PS, Lloyd D, Clark CA, Barker GJ, Parker GJM, McConville P, Baldock C, Pope JM (2000) Magn Reson Med 43:368–374
28. Heyes DM, Cass MJ, Powles JG, Evans WAB (2007) J Phys Chem B 111:1455–1464
29. Yeh IC, Hummer G (2004) J Phys Chem B 108:15873–15879